Numerical and theoretical studies of turbulence and transport with $\boldsymbol{E} \times \boldsymbol{B}$ shear flows

Z. Lin, M.S. Chance, T.S. Hahm, J.A. Krommes, W.W. Lee, I. Manuilskiy, H.E. Mynick, H. Qin, G. Rewoldt, W.M. Tang, R.B. White

Princeton Plasma Physics Laboratory,
Princeton University,
Princeton, New Jersey,
United States of America

Abstract. A report is given of: (a) a substantial transport reduction by the turbulence driven $\boldsymbol{E} \times \boldsymbol{B}$ flows observed in three dimensional non-linear gyrokinetic simulations of microturbulence in magnetically confined toroidal plasmas; (b) an analytical derivation of the effective shearing rate for the time dependent $\boldsymbol{E} \times \boldsymbol{B}$ flow; (c) an interpretation of experimental data using linear gyrokinetic microinstability rotation models of $\boldsymbol{E} \times \boldsymbol{B}$ shear; (d) other developments in gyrokinetic theory and simulation.

1. Introduction

There is accumulating evidence that $\boldsymbol{E} \times \boldsymbol{B}$ flow shear suppression of turbulence is the mechanism most likely to be responsible for various forms of confinement enhancement in magnetically confined plasmas. Understanding the mechanisms of turbulence suppression and discovering techniques to control turbulence are needed for developing magnetic fusion. Recent experimental data [1] from the core region of tokamaks have revealed the presence of small radial scale $\boldsymbol{E} \times \boldsymbol{B}$ flows that cannot be explained by the existing neoclassical theory. These observations point to the possibility that $\boldsymbol{E} \times \boldsymbol{B}$ flows are generated spontaneously and regulate the turbulence. Turbulent transport is believed to arise from electrostatic pressure gradient driven instabilities. These highly complex non-linear phenomena can be effectively investigated by numerical experiments. One of the most promising approaches is gyrokinetic particle simulation. Our gyrokinetic simulations [2] found a substantial reduction of heat transport due to turbulence generated $\boldsymbol{E} \times \boldsymbol{B}$ flows. These simulations of ion temperature gradient turbulence retained gyrokinetic ion dynamics and assumed an adiabatic electron response. We have also found that zonal flow structure plays a crucial role in causing the outstanding differences between global and local simulation results. The effective shearing rate for time dependent $\boldsymbol{E} \times \boldsymbol{B}$ flow is derived [3]. It is shown that the high frequency components of zonal flows are not effective in reducing turbulence. Finally, an improved rotation model for linear microinstability calculations is described and applications to experimental data are presented [4].

2. Gyrokinetic simulations of turbulence driven $\boldsymbol{E} \times \boldsymbol{B}$ flows

We have developed a fully three dimensional global gyrokinetic toroidal code (GTC) [2] for studying both turbulence and neoclassical physics [5]. The code uses a general geometry Poisson solver and Hamiltonian guiding centre equations of motion in magnetic co-ordinates to treat both advanced axisymmetric and non-axisymmetric configurations using realistic numerical MHD equilibria. This global code, which takes into account equilibrium profile variation effects, has low particle noise. Using a non-spectral Poisson solver [6], the equilibrium quantities, such as gyroradius and speed of sound, are allowed to be spatially dependent. In the simulations reported here, these equilibrium parameters are assumed to be uniform based on a two scale expansion. Furthermore, a single code can simulate both a full poloidal cross-section and an annular box in order to provide a connection between global and local simulations. The GTC code was implemented as a platform independent program and achieved nearly perfect scalability on various massively parallel processing (MPP) systems (e.g. an increase of speed by a factor of about 350 on a 512 node Cray-T3E computer).

Rosenbluth and Hinton [7] emphasized the importance of an accurate prediction of the undamped component of turbulence generated poloidal flows in determining the transport level in non-linear turbulence simulations and provided an analytical test for predicting the residual flow level in response to an initial flow perturbation. We reproduced this test in gyrokinetic particle simulations by solving the collisionless toroidal gyrokinetic equation with an initial source that is constant on a flux surface and introduced a perturbation of the poloidal flow. This flow was relaxed through the transit time magnetic pumping effect, followed by a slower damped oscillation with a characteristic frequency corresponding to that of the geodesic acoustic mode (GAM). The residual level of this flow measured from the simulation agrees well with the theoretical prediction. In the non-linear simulations of toroidal ITG instabilities, the $\boldsymbol{E}\times\boldsymbol{B}$ flows can be generated non-linearly by the Reynolds stress [8]. Our global simulations clearly demonstrate the existence and the importance of such self-generated flows, in qualitative agreement with flux tube simulations [9, 10]. These simulations used representative parameters [2] of DIII-D H mode core plasmas. The size of the plasma column was $a = 160\rho_i$. The simplified physics model includes an electron response of $\delta n_e/n_0 = e(\Phi - \langle\Phi\rangle)/T_e$, where $\langle\cdots\rangle$ represents the flux surface average. In a typical non-linear simulation, we calculated 5000 time steps of the trajectories of 100 million guiding centres interacting with the self-consistent turbulent field, which was discretized by 25 million ($128\times768\times256$) grid points in a three dimensional configuration. The instabilities evolved from a linear phase of growth to non-linear saturation with a peak transport level and finally to fully developed turbulence with a steady state transport level that is insensitive to initial conditions. To illustrate the effects of these flows on transport, we also carried out simulations of the same set of parameters with $\boldsymbol{E}\times\boldsymbol{B}$ flows suppressed by forcing $\langle\Phi\rangle = 0$. Comparison of the time history of χ_i from the simulation with turbulence driven $\boldsymbol{E}\times\boldsymbol{B}$ flows included with that from the simulation with the flows suppressed shows that a significant reduction (up to an order of magnitude) in the steady state ion heat conductivity occurs when $\boldsymbol{E}\times\boldsymbol{B}$ flows are retained.

A key mechanism for reducing transport by $\boldsymbol{E}\times\boldsymbol{B}$ flows is the breaking of turbulent eddies and, consequently, the reduction of the radial correlation length [11, 12]. This effect is visualized in a comparison of the poloidal contour plots of the fluctuation potential in the non-linear phase from a broad pressure profile simulation carried out with $\boldsymbol{E}\times\boldsymbol{B}$ flows included with one with the flows suppressed (Fig. 1). In both

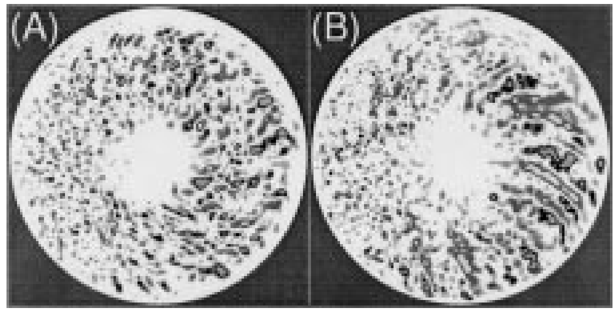

Figure 1. Poloidal contour plots of fluctuation potential $e\Phi/T_i$ in the steady state of a non-linear global simulation with $\boldsymbol{E}\times\boldsymbol{B}$ flows (a) included and (b) suppressed.

cases, the amplitude of fluctuations is highest at larger major radius where the drive of instabilities is strongest due to a bad magnetic curvature. Similar structures are observed in the linear phase for both cases. In the non-linear saturation stage $\boldsymbol{E}\times\boldsymbol{B}$ flows, which are linearly stable, are generated through an inverse cascade of spectrum [13] and begin to tear apart the turbulent eddies. In steady state, the fluctuations are observed to be nearly isotropic in the radial and poloidal directions when $\boldsymbol{E}\times\boldsymbol{B}$ flows are included in the simulations, whereas the turbulent eddies are elongated along the radial direction when the flows are suppressed. The fact that the breaking of turbulent eddies by $\boldsymbol{E}\times\boldsymbol{B}$ flows results predominantly in the reduction of the radial correlation length is also reflected in the observed flow induced broadening of the radial spectrum k_r of fluctuations [3]. These trends are in qualitative agreement with theoretical predictions [11, 12]. We also observed that this flow induced broadening of the k_r spectrum is accompanied by a reduction in fluctuation level, although we have not studied the relation between them in detail. Finally, the $\boldsymbol{E}\times\boldsymbol{B}$ flows also broaden the frequencies spectrum of individual modes, which would otherwise possess a coherent mode history corresponding to a frequency spectrum with a well-defined peak.

Fluctuating flows with a radial characteristic length comparable to that of the ambient turbulence have been generated in flux tube simulations [9, 10]. On the other hand, $\boldsymbol{E}\times\boldsymbol{B}$ flows with scale lengths of the order of the system size have been the dominant feature in previous global gyrokinetic simulations, although finer scale flows began to appear with larger system size [14]. These fundamentally different trends have been attributed to differences between global and local simulation models. Specifically, the whole plasma volume is simulated in global codes with pressure gradient profile variation and fixed boundary conditions, whereas local codes have a simulation domain that covers a few turbulent decorrelation lengths with a uniform pressure gradient and usually utilize radially periodic boundary conditions. We carried out simulations using both global and annular geometry with a variety of boundary conditions to address these differences. The perturbed electrostatic potential was set to zero at the boundary in all global simulations, and a radially periodic boundary condition was implemented in the annulus simulations. The profile of the pressure gradient was varied in the global simulations to distinguish the effects of profile variations from those of boundary conditions. When the profile of the pressure gradient was broad in the global simulations, the dominant components of the $\boldsymbol{E}\times\boldsymbol{B}$ flows have radial characteristic scale lengths comparable to the turbulence decorrelation length and characteristic frequencies comparable to those of the turbulence. Similar structures for the $\boldsymbol{E}\times\boldsymbol{B}$ shearing rate and good agreement between ion heat conductivities were obtained for the local and global simulations (within 20%). These results indicate that the periodic boundary conditions in local codes are not responsible for the differences between the trends observed in local and global simulations. As the variation in the pressure gradient becomes stronger in the global simulation, a static single well structure in the radial electric field, similar to those observed in previous global codes [14], emerges and becomes dominant. The ion heat conductivities also decrease because of the profile variation effects. We conclude that the narrow pressure gradient profile in global codes is responsible for the differences with the local code results.

3. Shearing rate of time dependent $\boldsymbol{E}\times\boldsymbol{B}$ flow

To address the reduction of turbulence in the presence of zonal flows, we consider a model problem in which the potential Φ associated with the zonal flows is a time dependent flux function, $\Phi(\psi,t) = \Phi_0(\psi)\exp[-i\omega_f(t-t_0)]$, with the corresponding radial shear of the angular frequency, $\Omega_\psi \equiv -\partial^2\Phi_0(\psi)/\partial^2\psi$. A two point correlation evolution equation is then derived following the procedure described in Ref. [3]. Results show that the radial correlation length Δr is reduced by the flow shear relative to its value Δr_0 determined by ambient turbulence alone: $(\Delta r_0/\Delta r)^2 = 1+\omega_{\mathit{eff}}^2/\Delta\omega_T^2$, where $\Delta\omega_T$ is the decorrelation rate of ambient turbulence and

$$\omega_{\mathit{eff}} \equiv \omega_E^{(0)} \frac{[(1+3F)^2+4F^3]^{1/4}}{(1+F)\sqrt{(1+4F)}}$$

is the effective shearing rate. Here, $F \equiv \omega_f^2/\Delta\omega_T^2$ and $\omega_E^{(0)} \equiv \Omega_\psi R B_\theta \Delta r_0/\Delta\phi$ is the instantaneous shearing rate, where $R\Delta\phi$ is the toroidal correlation length. We expect that a reduction of the fluctuations of the order of unity occurs if $\omega_{\mathit{eff}} \geq \Delta\omega_T$. When E_r varies slowly such that $F \ll 1$, we have $\omega_{\mathit{eff}} \sim \omega_E^{(0)}$, and recover the previous result in general toroidal geometry [10]. When E_r varies rapidly such that $F \gg 1$, we have $\omega_{\mathit{eff}} \ll \omega_E^{(0)}$, and turbulence suppression is difficult to achieve. This is because the flow pattern changes before eddies become distorted enough. This provides an explanation of our gyrokinetic simulation results [2], which show a considerable reduction, but not complete suppression, of turbulent transport although the instantaneous $\boldsymbol{E}\times\boldsymbol{B}$ shearing rate, part of which varies roughly on the turbulence timescale, is much larger than the maximum linear growth rate.

4. Linear microinstability rotation models

We have developed a more complete rotation model in the FULL [4] comprehensive linear microinstability code to assess the effect of $\boldsymbol{E}\times\boldsymbol{B}$ flows on the high-n toroidal drift modes destabilized by the combined effects of ion temperature gradients and trapped particles. This model allows a general flux co-ordinate toroidal geometry and includes contributions to the radial electric field from toroidal and poloidal rotations and from the ion pressure gradient. Application to TFTR enhanced reversed shear (ERS) cases confirms the well-known heuristic criterion for complete stabilization, i.e. that the $\boldsymbol{E}\times\boldsymbol{B}$ rotation shearing rate be greater than the linear growth rate without rotation. The implementation of this new (E_r) rotation model with the ballooning representation was described in some detail in Ref. [4]. A prescription for the ballooning parameter θ_0 is needed, in addition to the rotation model itself. The simplest choice, $\theta_0 = 0$, which is the usual choice in the absence of rotation, was employed in Ref. [3]. However, a better prescription can be determined as follows: one dimensional (ballooning representation) and two dimensional calculations for toroidal drift modes have been compared for the old rotation model in Ref. [15], and a way of modelling one of the missing two dimensional effects, 'eigenfunction shearing', in the one dimensional calculation was found there by modelling the 'average' or 'effective' value of θ_0 as a fitted function of the local Mach number. This additional 'eigenfunction shearing effect' decreases the maximum growth rate only moderately, and the radial marginal points where $\gamma = 0$ are barely moved. We conclude that including the two dimensional 'eigenfunction shearing' effect in the ballooning representation calculation changes the results only moderately.

5. Recent developments in gyrokinetic theory and simulation

A gyrokinetic system for arbitrary wavelength perturbations is derived using the phase space Lagrangian Lie perturbation method, which allows us to treat the background inhomogeneity and kinetic effects rigorously [16]. We have applied this self-consistent, comprehensive and fully kinetic approach to the study of MHD instabilities and electromagnetic drift waves. By decoupling the gyromotion from the particle gyrocentre orbit motion instead of averaging out the gyromotion, we have derived a gyrokinetic equation to describe the gyrokinetic perpendicular dynamics. This complete treatment of the perpendicular current enables us to recover the compressional Alfvén wave and arbitrary frequency modes, such as Bernstein waves from the gyrokinetic model.

We have devised an efficient and less noisy split weight δf scheme for treating electron dynamics in gyrokinetic simulations [17]. The response of each electron to the perturbations is split into an adiabatic and a non-adiabatic part. The evolution of the non-adiabatic part is followed dynamically and is determined by means of the continuity equation for perturbed charge density and current. This scheme has been validated for microinstability simulations in slab geometry.

The theory and implementation of the δf method for plasma simulation [18] are reconsidered. Statistical coarse graining techniques are used to give a rigorous derivation of the equation for the fluctuation δf in the particle distribution. It is shown that for dynamically collisionless situations a generalized thermostat or 'w stat' can be used in lieu of a full collision operator to absorb the flow of entropy to unresolved fine scales in velocity space and saturate the system.

6. Conclusions

Massively parallel global gyrokinetic particle simulations have demonstrated decorrelation of nonlinearly saturated turbulence and a reduction of associated transport by self-generated zonal flows. The effective shearing rate of these time dependent $\boldsymbol{E}\times\boldsymbol{B}$ flows has been derived analytically. Finally, linear microinstability calculations with an improved rotation model have been applied to experimental data.

Acknowledgements

This work has been supported by USDOE Contract No. DE-AC02-76CH03073 and in part by the Numerical Tokamak Turbulence Project.

References

[1] Bell, R., et al., Phys. Rev. Lett. **81** (1998) 1429.
[2] Lin, Z., Hahm, T.S., Lee, W.W., Tang, W.M., White, R.B., Science **281** (1998) 1835.
[3] Hahm, T.S., et al., Phys. Plasmas **6** (1999) 922.
[4] Rewoldt, G., et al., Phys. Plasmas **5** (1998) 1815.
[5] Lin, Z., Tang, W.M., Lee, W.W., Phys. Rev. Lett. **78** (1997) 456.
[6] Lin, Z., Lee, W.W., Phys. Rev. E **52** (1995) 5646.
[7] Rosenbluth, M.N., Hinton, F.L., Phys. Rev. Lett. **80** (1998) 724.
[8] Diamond, P.H., Kim, Y.B., Phys. Fluids B **3** (1991) 1626.
[9] Hammett, G.W., et al., Plasma Phys. Control. Fusion **35** (1993) 973.
[10] Dimits, A.M., et al., Phys. Rev. Lett. **77** (1996) 71.
[11] Biglari, H., Diamond, P.H. Terry, P.W., Phys. Fluids B **2** (1990) 1.
[12] Hahm, T.S., Burrell, K.H., Phys. Plasmas **2** (1995) 1648.
[13] Hasegawa, A., Wakatani, M., Phys. Rev. Lett. **59** (1987) 1581.
[14] Sydora, R.D., et al., Plasma Phys. Control. Fusion **38** (1996) A281.
[15] Rewoldt, G., et al., Phys. Plasmas **4** (1997) 3293.

[16] Qin, H., et al., Phys. Plasmas **5** (1998) 1035.
[17] Manuilskiy, I., et al., Bull. Am. Phys. Soc. **43** (1998) 1723.
[18] Krommes, J.A., Bull. Am. Phys. Soc. **42** (1997) 1982.

(Manuscript received 3 December 1998
Final manuscript accepted 5 May 1999)

E-mail address of Z. Lin: zlin@pppl.gov

Subject classification: D2, Tt